

Modeling of Long-Range Atmospheric Lasercom Links Between Static and Mobile Platforms

E. T. Scharlemann, E. F. Breidfeller, J. R. Henderson, J. S. Kallman, J. R. Morris, A. J. Ruggiero

This article was submitted to the "Society of Photo-Instrumentation Engineers (SPIE)" International Symposium on Optical Science and Technology, SPIE's 48th Annual Meeting, Free-Space Laser Communication and Active Laser Illumination III (AMIII), San Diego, CA, August 3-8, 2003

U.S. Department of Energy

Lawrence
Livermore
National
Laboratory

July 29, 2003

This document was prepared as an account of work sponsored by an agency of the United States Government. Neither the United States Government nor the University of California nor any of their employees, makes any warranty, express or implied, or assumes any legal liability or responsibility for the accuracy, completeness, or usefulness of any information, apparatus, product, or process disclosed, or represents that its use would not infringe privately owned rights. Reference herein to any specific commercial product, process, or service by trade name, trademark, manufacturer, or otherwise, does not necessarily constitute or imply its endorsement, recommendation, or favoring by the United States Government or the University of California. The views and opinions of authors expressed herein do not necessarily state or reflect those of the United States Government or the University of California, and shall not be used for advertising or product endorsement purposes.

This work was performed under the auspices of the U.S. Department of Energy by University of California, Lawrence Livermore National Laboratory under Contract W-7405-Eng-48.

Modeling of long-range atmospheric lasercom links between static and mobile platforms*

E. T. Scharlemann, E. F. Breittfeller, J. R. Henderson,
J. S. Kallman, J. R. Morris, and A. J. Ruggiero
Lawrence Livermore National Laboratory, L-183
Livermore, California 94550

ABSTRACT

We describe modeling and simulation of long-range terrestrial laser communications links between static and mobile platforms. Atmospheric turbulence modeling, along with pointing, tracking and acquisition models are combined to provide an overall capability to estimate communications link performance.

Keywords: free-space optical communications, atmospheric turbulence, pointing, tracking, and acquisition

1. INTRODUCTION

The SATRN (Secure Air-Optic Transport and Routing Network) project^{1,2} at LLNL is pursuing a series of laser communication experiments between ground-based and airborne platforms at long ranges. Modeling of these experiments requires combining pointing, tracking, and acquisition models with models describing the effects of atmospheric turbulence in order to have a chance of reproducing the performance of the communications links.

One approach to modeling the communication link involves simulated propagation – via two-dimensional FFTs – of coherent light through phase screens representing turbulent layers. This approach is very useful for evaluating turbulence contributions to beam spread, and for estimating the scintillation index, aperture averaging factors, and the loss incurred in coupling turbulence-distorted light into single mode fibers.³ The approach is much less useful for extensive calculations of communications link performance in terms of probability of fade or bit-error rate (BER); if the link is at all robust, the fades and bit-errors occur in the distant wings of the intensity probability distribution function (PDF). Additionally, coupling the phase-screen simulations to pointing and tracking error models is probably awkward.

Instead, our approach in this paper is to use a heuristic theory for scintillation⁴⁻¹¹ that has been extensively developed at the University of Central Florida (UCF) by L. Andrews, R. Phillips, and their collaborators. The virtue of this formulation of scintillation is in the direct connection between two parameters describing the turbulence and the receiver aperture that provides both an estimate of the scintillation index and an expression for the PDF of scintillated intensity, with and without aperture averaging. This intensity PDF can be coupled to the pointing and tracking model to arrive (at least numerically) at an overall PDF for power in the receiver aperture, and hence estimates of BER and fade probability.

In addition, atmospheric transmission values are calculated with FASCODE^{12,13} and HITRAN 2000^{14,15} (the spectral line database used by FASCODE).

2. THE UCF SCINTILLATION MODEL – A SUMMARY

The heuristic scintillation model appears in many forms, but begins with

$$\sigma_1^2 = 1.23 C_n^2 k^{7/6} L^{11/6}, \quad (1)$$

the Rytov variance for a plane wave in weak scintillation theory. The parameter characterizing the receiver aperture diameter – and hence aperture averaging effects – is

$$d^2 = \frac{k D^2}{4L}. \quad (2)$$

*To be published in Proc. SPIE 5160 (2003).

The effect of strong turbulence is pictured⁵ in terms of small-spatial-scale fluctuations modulating large-scale fluctuations, with the large-scale and small-scale fluctuations statistically independent. The two scales are implemented mathematically by inserting heuristic spatial-frequency filters into weak-turbulence integrals for scintillation index. Appropriate scale factors are then chosen to ensure the proper weak-turbulence and asymptotic strong-turbulence limits. The contribution of large-scale fluctuations to the scintillation index σ_I^2 is denoted by σ_x^2 , the small scale contribution by σ_y^2 , and

$$\sigma_I^2 \equiv \frac{\langle I^2 \rangle}{\langle I \rangle^2} - 1 = (1 + \sigma_x^2)(1 + \sigma_y^2) - 1. \quad (3)$$

The quantities σ_x^2 and σ_y^2 are obtained from the integral with large-scale spatial frequency filter, $\sigma_{\ln x}^2$, and the integral with small-scale spatial frequency filter, $\sigma_{\ln y}^2$. In terms of these last two quantities

$$\sigma_x^2 = e^{\sigma_{\ln x}^2} - 1, \quad \sigma_y^2 = e^{\sigma_{\ln y}^2} - 1, \quad \text{and} \quad \sigma_I^2 = \exp(\sigma_{\ln x}^2 + \sigma_{\ln y}^2) - 1. \quad (4)$$

For the specific application here, we work with the spherical wave model with aperture averaging modifications,⁶ for which two additional intermediate quantities appear in the integrals:

$$\eta_x = \frac{8.56}{1 + 0.186\sigma_1^{12/5}} \quad (5)$$

and

$$\eta_y = 9(1 + 0.23\sigma_1^{12/5}). \quad (6)$$

In terms of these,

$$\sigma_{\ln x}^2 = \frac{0.016\sigma_1^2\eta_x^{7/6}}{(1 + 0.021d^2\eta_x)^{7/6}} \quad (7)$$

and

$$\sigma_{\ln y}^2 = \frac{1.272\sigma_1^2\eta_y^{-5/6}}{1 + 0.1d^2\eta_y}. \quad (8)$$

The PDF of intensity in scintillations is represented by a ‘‘gamma-gamma’’ function⁹ characterized by two parameters, α and β , with

$$P(I) = \frac{2(\alpha\beta)^{(\alpha+\beta)/2}}{\Gamma(\alpha)\Gamma(\beta)} I^{(\alpha+\beta)/2-1} K_{\alpha-\beta} \left[2(\alpha\beta I)^{1/2} \right] \quad \text{for which} \quad \langle I \rangle = 1. \quad (9)$$

The charm of the UCF scintillation model is that the two parameters in the gamma-gamma distribution are related to the turbulence integrals through

$$\alpha = \frac{1}{\sigma_x^2}, \quad \beta = \frac{1}{\sigma_y^2}. \quad (10)$$

The disadvantage of this spherical wave model with aperture averaging is that it is intended only to apply to propagation paths with constant C_n^2 , and does not account for any off-axis increase in scintillation index.¹⁰ At least as of this writing (to the authors’ knowledge), a Gaussian-beam model with aperture averaging corrections is not yet available, nor is a variable C_n^2 model with aperture averaging.

With this model for scintillation and for the intensity PDF, it is possible to choose a propagation path (preferably approximately constant C_n^2) and a receiver aperture size and arrive at a workable form for intensity PDF and a value for scintillation index at the receiver.

3. PLATFORM MOTION MODELING

We have developed a 6-degree-of-freedom simulation to model the dynamics of a platform-mounted two-axis gimbal in order to evaluate the pointing and tracking performance. The gimbal, in this case roughly modeled to represent Wescam's 14" Skyball, is assumed mounted on (for the example considered below) two platforms; a mid-altitude aircraft (Sabreliner) at 30,000 ft and a high-flying aircraft at 60,000 ft. Skyball specifications were used to derive the properties of its active controller and passive isolation system. Each axis (azimuth, elevation) of both the active controller and passive isolation system is represented by a second-order transfer function. Experimental vibration data is used to model the dynamic flight response of the aircraft as an N^{th} -order transfer function, where N depends on the aircraft. Track Kalman filters are included to enable automatic beam reacquisition following loss-of-lock. Loss-of-lock conditions are defined as obscuration of the line-of-sight (LOS) and are randomly imposed throughout the simulation on each path of the communication link. Two pointing and tracking control algorithms have been investigated: a) direct detection, and b) nutating. Various engagement geometries have been simulated in order to arrive at a one-dimensional Rician pointing error probability distribution. The engagements vary from non-stressing to stressing, thus permitting an examination of tracking performance across a range of LOS dynamics.

Each aircraft is modeled by the following 13-element state vector \vec{X}_{AC} :

$$\vec{X}_{AC} = [\vec{q}_{4 \times 1}^T \quad \vec{\omega}_{3 \times 1}^T \quad \vec{r}_{3 \times 1}^T \quad \vec{v}_{3 \times 1}^T] \quad (11)$$

where \vec{q} is quaternion, $\vec{\omega}$ is angular rate, \vec{r} is position, and \vec{v} is velocity.

Attitude and guidance closed-loop controllers are included so that the aircraft will follow the desired flight plan (e.g., perform a figure with standard rate turns). Additionally the aircraft angular body rates, $\vec{\omega}$, are subjected to aerodynamic disturbance torques that are modeled based upon the experimental vibration data. These disturbance torques have the effect of degrading the performance of the attitude control system, which ultimately are felt (act as a forcing function) by the aircraft-mounted Skyball, thus affecting pointing accuracy. Fig. 1 shows a sample frequency response of the Sabreliner disturbance torques for a given flight regime.¹⁶

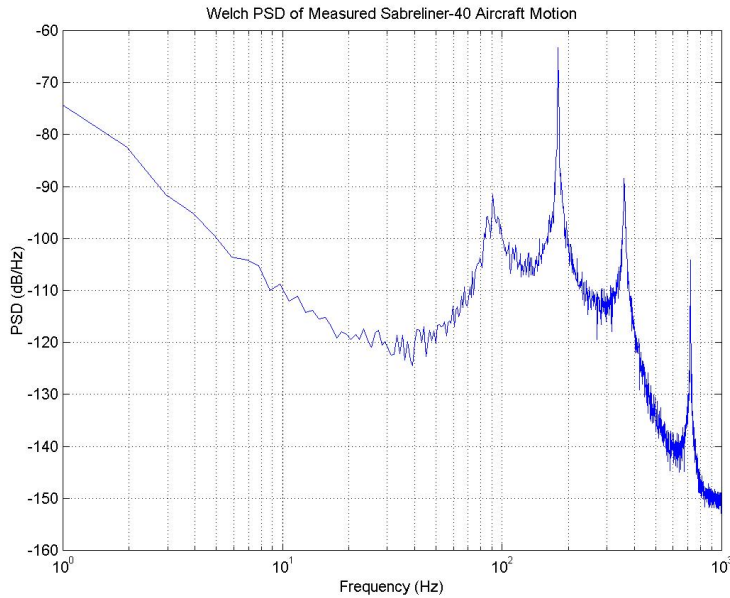


Figure 1: Sample frequency response of Sabreliner aircraft

An N^{th} -order transfer function is chosen which approximates the first three resonant modes as well as matching the low frequency response.

The skyball is a two-axis servo-controlled gimbal with passive isolation. The active and passive control responses are modeled with 2nd-order transfer functions, each with varying parameters as specified by the manufacturer. The 8-element skyball state vector is defined as

$$\vec{X}_{SB} = \left[\vec{A}_{SB,4 \times 1}^T \vec{P}_{SB,4 \times 1}^T \cdot \right] \quad (12)$$

with \vec{A} the active portion and \vec{P} the passive.

The aggregate continuous-time 21x1 state vector of a system describing a skyball mounted on an aircraft frame is therefore defined as

$$\vec{X}_{AS} = \left[\vec{q}_{4 \times 1}^T \vec{\omega}_{3 \times 1}^T \vec{r}_{3 \times 1}^T \vec{v}_{3 \times 1}^T \vec{A}_{SB,4 \times 1}^T \vec{P}_{SB,4 \times 1}^T \right] \quad (13)$$

Numerical integration of the state vector is done using a 4th-order variable-step-size Runge-Kutta integrator.

The target-track Kalman filter is implemented on each side of the two-way communications link (e.g., one track filter inside a skyball on the high-altitude aircraft tracking the Sabreliner, and another track filter in a Sabreliner-mounted skyball tracking the high-altitude aircraft). The 9-element discrete-time track filter state vector, \vec{X}_{TF} , is defined as

$$\vec{X}_{TF} = \left[\Delta \vec{x}_{3 \times 1}^T \Delta \vec{v}_{3 \times 1}^T \Delta \vec{a}_{3 \times 1}^T \right] \quad (14)$$

where the states are relative positions (\vec{x}), velocities (\vec{v}), and accelerations (\vec{a}). The filter is generic, yet useful for generating baseline metrics. Other filter implementations are available and can be chosen depending upon the specific application. The measurement inputs to the Kalman filter are the high accuracy LOS (measured by the Skyball and transformed to the inertial frame).

The purpose of the track filter is to enable automatic reacquisition following some period of LOS obscuration or signal fadeout. Provided that the dropout time is not too long, the tracking system should still have the target either a) within its narrow FOV telescope, or b) within its wide FOV camera, once the obscuration passes or the signal fadeout ends. This eliminates the burden of a time-consuming, and perhaps unsuccessful, search and reacquisition phase. During a loss-of-lock condition, the track filter propagates its state vector forward in time to provide an estimated pointing vector to the tracking system.

Two variations of deriving a commanded pointing vector have been implemented: a) position sensitive (direct) detection, and b) nutation (synchronous) detection. Both versions derive a commanded pointing vector, and then pass this command to a proportional-integral-derivative (PID) controller. Other controllers are available, but the PID implementation is viewed as providing a standard baseline metric. Only direct detection will be discussed here: it is modeled as derived from the linear position of the laser light's incident position on a two-dimensional X-Y detector surface, and thus directly provides the pointing error. The primary potential benefit of the nutational method results from the fact that the nutated beam may be synchronously demodulated, which may yield better signal detection in the presence of optical background clutter than the direct detection method.¹⁷⁻¹⁹

An example of tracking error derived from this model is shown in Fig. 2 for 100-km propagation from the high-flying aircraft to the Sabreliner. The high-flyer is modeled as a more stable version of the Sabreliner. A four-second segment is shown on the left, and a higher resolution (in time) segment on the right.

4. LINK-PERFORMANCE MODELING

The pointing offset and jitter illustrated in Fig. 2 can be folded into scintillation modeling with a four-step process involving three integrals of conditional probabilities to obtain an intensity PDF $P(I)$, varying with time, and a final integral over $P(I)$ to convert that to a probability of error, or instantaneous bit-error rate. We treat the pointing trajectory of Fig. 2 as a time-varying average pointing offset with a small pointing jitter (Gaussian PDF with $\sim 0.5 \mu\text{rad}$ rms) superimposed. At each positional offset (x_c, y_c) at the receiver, there is a PDF for the actual radial offset r from beam center given by

$$P(r) = \int_{-\infty}^{\infty} P(r|x)P(x) dx, \quad (15)$$

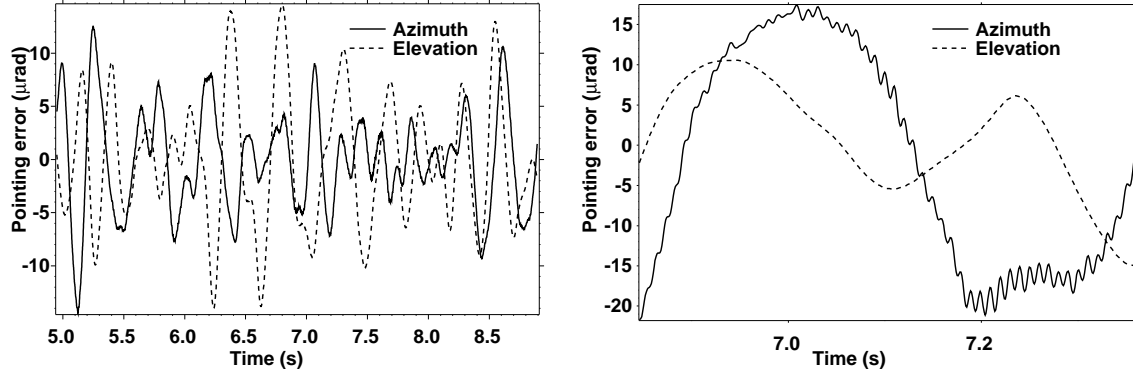


Figure 2: Modeled pointing error vs time for a high-flying aircraft to a mid-altitude aircraft

where

$$P(x) = \frac{1}{\sqrt{2\pi} \sigma_x} e^{-(x-x_c)^2/2\sigma_x^2} \quad (16)$$

and

$$P(r|x) = \frac{r}{\sqrt{2\pi(r^2-x^2)} \sigma_y} e^{-[(\sqrt{r^2-x^2}-y_c)^2/2\sigma_y^2]} \quad (17)$$

As the pointing of the (on average) Gaussian beam varies, the average intensity $\langle I \rangle$ at the receiver varies correspondingly, with a PDF for $\langle I \rangle$ of

$$P(\langle I \rangle) = \frac{w_e^2}{2r\langle I \rangle} P(r), \quad (18)$$

where r is determined by $I(r) = \langle I \rangle$, and w_e is the $1/e^2$ -intensity radius of the Gaussian beam after diffractive and turbulent beam spread.

Then, for instantaneous beam intensity in the presence of scintillation,

$$P(I) = \int_0^\infty P(I|\langle I \rangle) P(\langle I \rangle) dI \quad (19)$$

where $P(I|\langle I \rangle)$ is the gamma-gamma distribution of Eq. 9.

Finally, with this $P(I)$ that folds in pointing offset and jitter as well as scintillation, a probability of bit error can be found for a given average SNR from⁸ (for on-off keying [OOK])

$$P(E) = \int_0^\infty P(I) \operatorname{erfc} \left[\frac{\langle SNR \rangle I}{2\sqrt{2}\langle I \rangle} \right] dI \quad (20)$$

and erfc is the complementary error function.

5. A LONG-RANGE AIR-TO-AIR EXAMPLE

With the pointing error and jitter of Fig. 2, it is possible to apply the BER modeling to evaluate an example of communications link performance at the 100-km range of the figure. Fig. 3a shows the resulting short-time average beam offset at the Sabreliner.

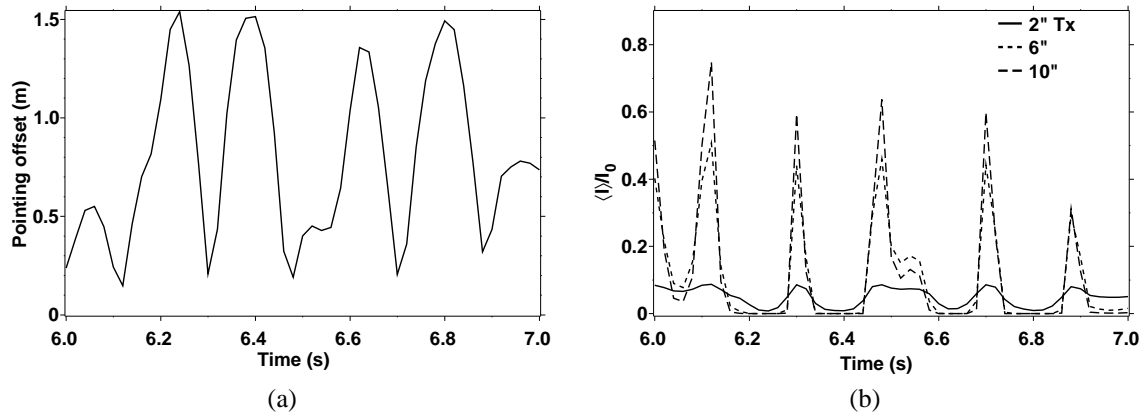


Figure 3: Beam offset and average normalized beam intensity at target vs time over a one-second interval

At $1.55 \mu\text{m}$ and with a C_n^2 of $10^{-17} \text{ m}^{-2/3}$ (typical of most average turbulence models at high-altitude), and for a collimated beam from several transmitter diameters, the resulting average (unscintillated but jittered) intensity at the target is shown in Fig. 3b. The intensity is normalized to the peak intensity (with turbulent beam spread, but no jitter and no pointing error) of the collimated beam from the 10" transmitter. For the range and C_n^2 used, $\sigma_1^2 \approx 1$. For the spherical wave model with aperture averaging, $\alpha = 8.93$ and $\beta = 6.71$ in the gamma-gamma distribution.

The final instantaneous probability of OOK bit error is shown in Fig. 4, for a SNR of 100 (20 dB) at the peak intensity of the beam from the 10" aperture. At this very long range, and with the pointing and tracking stability as modeled, only short intervals – when the beam is pointed best – achieve reasonable levels of performance (low BER), and then only for the larger transmitter apertures.

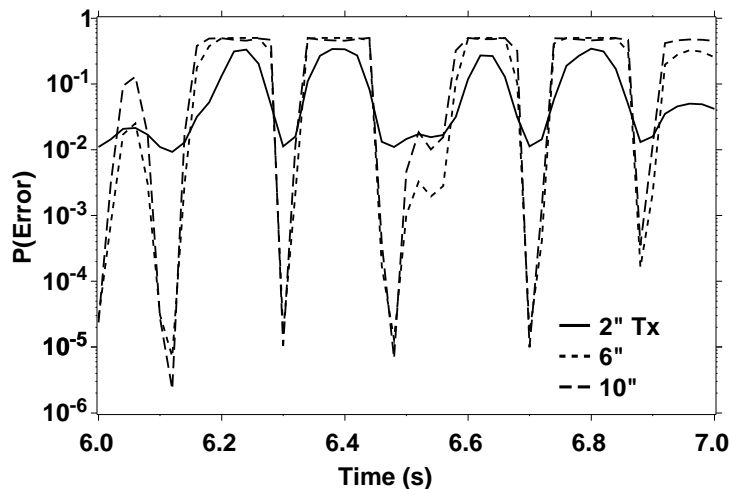


Figure 4: Probability of bit error at the target vs time over a one-second interval

6. DISCUSSION AND FUTURE WORK

The model we have put together is not yet complete. Potential complications that have not been incorporated are

- path-varying C_n^2 for uplink or downlink paths,
- inner and outer scale effects (and unknown inner and outer scales),
- aircraft boundary-layer turbulence effects,
- statistics of coupling of received signal to fiber mode,
- off-axis scintillation terms, and
- the effects of adaptive optics, which are included in the data collections.

Additionally, the fact that the C_n^2 profile, and both the inner and outer scales of turbulence, will not be completely characterized greatly complicates comparisons of the model with experimental data.

Nevertheless, the SATRN project is generating large amounts of data, and the focus of the modeling work will be on bringing the integrated model into approximate agreement with the data.

ACKNOWLEDGMENTS

This work was performed under the auspices of the US Department of Energy by Lawrence Livermore National Laboratory under contract W-7405-ENG-48.

REFERENCES

1. G. W. Johnson, J. P. Cornish, J. W. Wilburn, R. A. Young, and A. J. Ruggiero, "Characterization of Gigabit Ethernet over highly turbulent optical wireless links," Proc. SPIE **4821**, 283-290, 2002.
2. C. A. Thompson, M. W. Kartz, L. M. Flath, S. C. Wilks, R. A. Young, G. W. Johnson, and A. J. Ruggiero, "Free space optical communications utilizing MEMS adaptive optics correction," Proc. SPIE **4821**, 129-138, 2002.
3. S. C. Wilks, J. R. Morris, J. M. Brase, S. S. Olivier, J. R. Henderson, C. A. Thompson, M. W. Kartz, and A. J. Ruggiero, "Modeling of adaptive optics based free-space communications systems," Proc. SPIE **4821**, 121-128, 2002.
4. L. C. Andrews and R. L. Phillips, *Laser Beam Propagation through Random Media*, SPIE Optical Engineering Press, Bellingham WA, 1998.
5. L. C. Andrews, R. L. Phillips, C. Y. Hopen, and M. A. Al-Habash, "Theory of optical scintillation," *J. Opt. Soc. Am.* **A16**, 1417-1429, 1999.
6. L. C. Andrews, R. L. Phillips, and C. Y. Hopen, "Aperture averaging of optical scintillations: power fluctuations and the temporal spectrum," *Waves in Random Media* **10**, 53-70, 2000.
7. L. C. Andrews, R. L. Phillips, and C. Y. Hopen, "Scintillation model for a satellite communication link at large zenith angles," *Opt. Eng.* **39**, 3272-3280, 2000.
8. L. C. Andrews, R. L. Phillips, and C. Y. Hopen, *Laser Beam Scintillation with Applications*, SPIE Optical Engineering Press, Bellingham WA, 2001.
9. M. A. Al-Habash, L. C. Andrews, and R. L. Phillips, "Mathematical model for the irradiance probability density function of a laser beam propagating through turbulent media," *Opt. Eng.* **40**, 1554-1562, 2001.
10. L. C. Andrews, M. A. Al-Habash, C. Y. Hopen, and R. L. Phillips, "Theory of optical scintillation: Gaussian-beam wave model," *Waves in Random Media* **11**, 271-291, 2001.
11. L. C. Andrews and R. L. Phillips, "Impact of scintillations on laser communication systems: recent advances in modeling," Proc. SPIE **4489**, 23-34, 2002.
12. S. A. Clough, F. X. Kneizys, G. P. Anderson, E. P. Shettle, J. H. Chetwynd, and L. W. Abreu, "FASCOD3: Spectral Simulation", in *IRS '88: Current Problems in Atmospheric Radiation – Proceedings of the 1988 International Radiation Symposium*, ed., J. Lenoble and J.-F. Geleyn, Deepak Publishing, Hampton, VA, 1989.
13. G. P. Anderson, J. Wang, M. L. Hoke, F. X. Kneizys, J. H. Chetwynd, L. S. Rothman, L. M. Kimball, R. A. McClatchey, E. P. Shettle, S. A. Clough, W. O. Gallery, L. W. Abreu, and J. E. A. Selby, "History of One Family of Atmospheric Radiative Transfer Codes", Proc. SPIE **2309**, 170-183, 1994.
14. L. S. Rothman, R. R. Gamache, R. H. Tipping, C. P. Rinsland, M. A. H. Smith, D. C. Benner, V. M. Devi, J.-M. Flaud, C. Camy-Peyret, A. Perrin, A. Goldman, S. T. Massie, L. R. Brown, and R. A. Toth, "The HITRAN Molecular Database: Editions of 1991 and 1992," *J. Quant. Spectrosc. Radiat. Transfer* **48**, 469-507, 1992.

15. <http://cfa-www.harvard.edu/HITRAN/>
16. Sabreliner vibration data was kindly provided by Robert A. Gill, AFRL/SNJM, Wright Patterson AFB.
17. E. A. Swanson and V. W. S. Chan, "Heterodyne spatial tracking systems for optical space communication," IEEE Trans. Commun., **COM-34**, 118-126, 1986.
18. C-C. Chen and C. S. Gardner, "Impact of random pointing and tracking errors on the design of coherent and incoherent optical intersatellite communication links", IEEE Trans. On Commun., **37**, 252-260, 1989.
19. V. W. S. Chan and J. E. Kaufmann, "Coherent optical intersatellite crosslink systems," Proc. SPIE **988**, 325-335, 1989.